

# Two-sided conical laser target for a neutron source of a hybrid nuclear-thermonuclear reactor\*

I.G. Lebo, E.A. Isaev, A.I. Lebo

**Abstract.** Numerical simulations suggest that a source of thermonuclear neutrons with a high pulse repetition rate and the number of neutrons of  $\sim 10^{17}$  per pulse, which is required for the development of nuclear-thermonuclear reactors, can be realised in the irradiation of a two-sided conical target simultaneously by a long and short laser pulses with energies of  $\sim 1$  MJ and 50 kJ and durations of 100–250 ns and 0.1–1 ns. We consider the feasibility of verifying separate propositions of the proposed conception with the use of existing laser facilities.

**Keywords:** nuclear-thermonuclear reactor, laser source of thermonuclear neutrons, conical target.

## 1. Introduction

In the Russian Federation [1] and in several developed countries in the world (USA, France, and China) research is underway to make high-power lasers (drivers) for the initiation of thermonuclear microexplosions. The largest multi-channel neodymium-glass laser facility (Nd-laser) – NIF (National Ignition Facility) – has operated in the USA since 2012 [2]. In such facilities, thermonuclear microexplosions give rise to high-power fluxes of thermonuclear neutrons (with an energy  $\epsilon_n \approx 14$  MeV), charged particles (in particular,  $\alpha$  particles with an energy  $\epsilon_\alpha \approx 3.5$  MeV), and hard electromagnetic radiation. This source is of major interest for research in astrophysics and material science as well for other applied problems.

At the same time, the development of an Nd-laser based driver for a nuclear-thermonuclear reactor operating at a high repetition rate of microexplosions and having a long service life is highly disputable. The series-parallel configurations of pulse amplification in glass stages of different aperture (rods, plates, or disks) and the conversion of IR radiation to the second and third harmonic are responsible for additional energy loss and complicate attaining the uniform irradiation of a spherical target required for overcompression of deuterium–tritium (DT) fuel.

\* Reported at ECLIM 2016 (Moscow, 18–23 September 2016).

**I.G. Lebo** Moscow Technological University (MIREA), prosp. Vernadskogo, 78, 119454 Moscow, Russia; e-mail: lebo@mail.ru;  
**E.A. Isaev** National Research University Higher School of Economics, ul. Myasnitskaya, 20, 101000 Moscow, Russia;  
**A.I. Lebo** School No. 1329, ul. Nikulinskaya, 10, 119602 Moscow, Russia

Received 15 December 2016  
 Kvantovaya Elektronika 47 (2) 106–110 (2017)  
 Translated by E.N. Ragozin

High-power gas lasers, in particular KrF excimer lasers, offer a variety of advantages [3], which permit considering them as the drivers for hybrid nuclear-thermonuclear reactors [4, 5].

Figure 1 depicts a diagram of the energy cycle of a thermonuclear power station [6]. Here,  $\eta$  is the laser efficiency;  $G$  is the energy gain in the thermonuclear target;  $\beta$  is the thermal-to-electric energy conversion efficiency;  $\phi$  is the energy fraction which goes to provide the reactor operation;  $f$  is the laser pulse repetition rate;  $E_L$  is the pulse energy;  $W_t = fKE_L$  is the thermal power produced in the reactor;  $K = (0.2 + 0.8M)G$  is the total energy gain in the reactor;  $M$  is the energy multiplication factor in the uranium reactor blanket; and  $(1/\eta - 1)fE_L$  is the energy loss in the laser pumping, which may be partly employed for practical purposes.

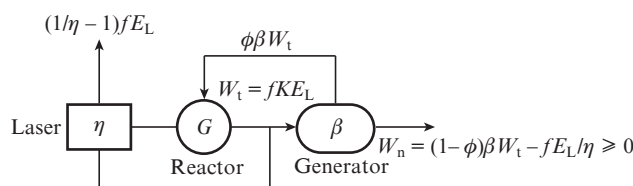


Figure 1. Energy cycle diagram of a thermonuclear power plant.

To close the energy cycle, the following inequality must be satisfied:

$$(1 - \phi)\beta(0.2 + 0.8M)G - 1/\eta > 0. \tag{1}$$

On can see from inequality (1) that this is extremely hard to achieve for a low  $\eta$ . For a KrF laser with a pulse duration of  $\sim 100$  ns it is possible to reach  $\eta \geq 0.05$ , which gives the hope, in principle, of closing the energy cycle even when  $G = 1$  (if use is made of enriched uranium in the blanket with  $M > 60$ ).

The authors of Refs [6, 7] proposed the use of conical targets and a KrF laser as a driver of a hybrid reactor. However, until the present time the emphasis was placed on the development of neodymium laser systems, because it is planned to obtain a high gain in the thermonuclear target ( $G \gg 1$ ). To obtain high  $G$  values and initiate the thermonuclear burn wave, the fuel must be compressed to a density 1000 times the density of a liquid DT mixture. Owing to the development of the hydrodynamic instability and mixing (for more details, see Refs. [8, 9]), attempts to provide these conditions in inertial thermonuclear fusion targets so far have not met with success. On the other hand, attaining  $G \approx 1$  is an independent task of high practical significance [10].

In this work we consider the feasibility of obtaining a gain  $G \approx 1$  in a two-sided conical thermonuclear target and closing the energy cycle of a hybrid power plant with the use of a KrF laser operating in the regime of long and short pulse generation [11]. As shown by our numerical simulations, to do this requires UV lasers with a pulse energy of  $\sim 1$  MJ, it being sufficient to compress condensed fuel (a liquid DT mixture) by a factor of 30–50. The whole compression proceeds under the action of the incident and reflected shock waves, and in these conditions one might expect that mixing would not lead to a catastrophic situation, i.e. to a decrease of the neutron yield by several orders of magnitude in comparison with the yield resulting from one-dimensional simulations.

## 2. Formulation of the problem

The target heating and compression were simulated using the two-dimensional Atlant\_Sp code on spherical Lagrangian coordinates  $(r, \theta)$  [8, 9]. Given below is the system of plasma-dynamic equations which underlay this code:

$$\begin{aligned} \frac{d\rho}{dt} &= -\rho \operatorname{div} V, \\ \rho \frac{dV}{dt} &= -\operatorname{grad} p, \quad p = p_i + p_e, \\ \rho \frac{d\varepsilon_i}{dt} &= -p_i \operatorname{div} V + \operatorname{div}(\kappa_i \operatorname{grad} T_i) + C_i \rho \frac{T_e - T_i}{\tau_{ei}} + \Delta E_{fi}, \\ \rho \frac{d\varepsilon_e}{dt} &= -p_e \operatorname{div} V + \operatorname{div}(\kappa_e \operatorname{grad} T_e) \\ &\quad - C_i \rho \frac{T_e - T_i}{\tau_{ei}} + \operatorname{div} q_L + \Delta E_{fe}. \end{aligned} \quad (2)$$

Here,  $\rho$  is the density,  $V$  is the velocity;  $p_e, p_i, T_e, T_i, \varepsilon_e, \varepsilon_i$  and  $\kappa_e, \kappa_i$  are the pressures, temperatures, specific internal energies, and nonlinear heat conductivity coefficients of the electron and ion plasma components, respectively;  $C_i$  is the thermal capacity of the ion component;  $\tau_{ei}$  is the electron–ion relaxation time; and  $q_L$  is the laser radiation flux. In the simulations it was assumed that laser radiation propagated strictly radially (along the generatrix of the conical target), was absorbed by inverse bremsstrahlung, and was absorbed in the corresponding Lagrangian cell on reaching the critical surface. The physicomathematical model implied that the equation of state corresponded to a fully ionised ideal plasma and the transfer coefficients were classical [12].

The simulations by the Atlant\_Sp code also included the local transfer of the energies  $\Delta E_{fe}$  and  $\Delta E_{fi}$  from charged thermonuclear particles (primarily,  $\alpha$  particles) to the electron and ion plasma components, respectively\*.

Figure 2 shows the structure of a two-sided conical target. The sections of target channels are truncated cones ( $R_{\min}$  and  $R_0$  are the radii at the summit and at the base). Near the channel summits is the DT mixture in the form of a frozen layer of radius  $R_2$ ; located next are a layer of low-density DT vapour of thickness  $R_1 - R_2$ , a thin dense polymer ‘tamper’ layer of thickness  $\Delta_{\text{CH}}$ , an absorber layer of a low-density material and, at the outer side, a thin film of thickness  $0.5 \mu\text{m}$ . The total absorber thickness is  $R_0 - R_1$ . The averaged absorber

density  $\rho_3 = 10 \text{ mg cm}^{-3}$ , the polyethylene density  $\rho_{2(4)} = 1 \text{ g cm}^{-3}$ , the frozen DT mixture density  $\rho_6 = 0.25 \text{ g cm}^{-3}$ , and the DT vapour density  $\rho_5 = 5 \mu\text{g cm}^{-3}$ . The outer walls should be made of a heavy material (for instance, gold). The angular cone aperture  $\alpha_0$  as well the radii  $R_0, R_1, R_2$ , and  $R_{\min}$  were treated as parameters of the problem and were varied. Our simulations implied that the channel walls were perfectly elastic and thermally insulated.

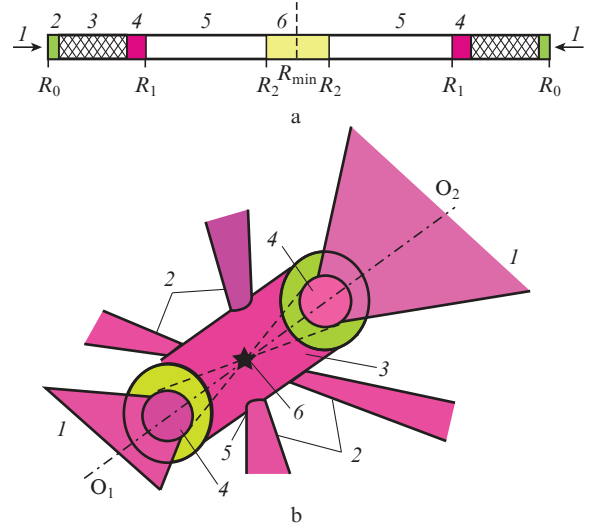


**Figure 2.** (a) Cross-sectional schematic diagram of a two-sided conical target [(1) long irradiation laser pulses; (2) thin polymer layer; (3) low-density absorber aerogel; (4) working polymer layer of thickness  $\Delta_{\text{CH}}$ ; (5) fuel vapour; (6) cryogenic DT mixture layer; the vertical dashed line shows the symmetry plane], (b) general view of this target [(1) long pulses; (2) short laser pulses propagating in the plane perpendicular to the axis of the conical channel  $O_1O_2$ ; (3) golden cylinder; (4) conical channels; (5) openings for the injection of short pulses; (6) thermonuclear microexplosion].

We simulated the compression of thermonuclear fuel by a long laser pulse. Two series of the simulations were performed. Used in the first series was a laser pulse duration  $\tau_L = 101 \text{ ns}$ , a pulse energy  $E_L = 1 \text{ MJ}$ , an angular cone aperture  $\alpha_0 = \pi/10$  (the temporal pulse shape is shown in Fig. 3a). In the second series,  $\tau_L = 251 \text{ ns}$ ,  $E_L = 1 \text{ MJ}$ , and  $\alpha_0 = \pi/12$  (the temporal pulse shape is shown in Fig. 3b).

In our simulations, the absorption of laser radiation was assumed to be equal to 100%.

To describe the energy transfer in the plasma produced in the interaction of a high-power laser pulse with a porous medium, use was made of the model developed in

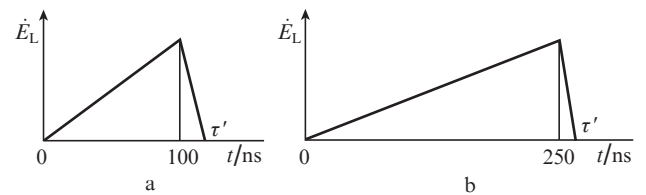


**Figure 3.** Temporal shapes of the laser pulses employed in (a) the first and (b) second series of simulations.

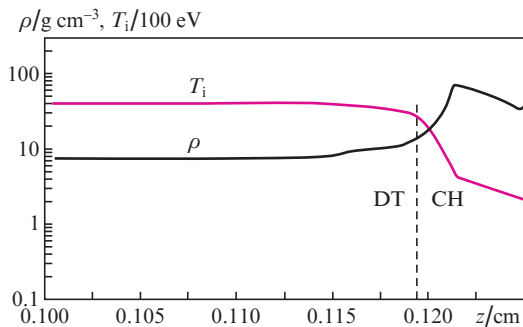
\*The physicomathematical model and the methods of solution of Eqns (2) are described in greater detail in Refs [8, 9, 13].

Refs [14–16]. This model is underlain by the following hypothesis. At the first stage of laser target irradiation, the substance remains almost transparent, since the volume occupied by the pore walls amounts to only  $10^{-2}$ – $10^{-3}$  of the entire material volume. The duration of this stage corresponds to the time of plasma formation  $t_1 \approx d/V_s$  ( $d$  is the pore size and  $V_s$  is the plasma sound velocity), i.e.  $t_1 \approx 0.1$ – $0.2$  ns. In order not to produce pressure perturbations directly at the tamper surface at the initial stage of the process, a thin layer of dense polyethylene of thickness  $\sim 0.5$   $\mu\text{m}$  was placed on the outer side of the porous layer. When the radiation passes through the porous material, a small fraction (no more than 1%) of the laser energy flux is absorbed in the pore walls and blows them up. In the evaporation and collision of pore walls there forms a turbulent plasma with a typical vortex size of the order of the pore size. Subsequently the radiation propagates through this turbulent plasma. By analogy with the Belen'kii–Fradkin turbulence model [17], we introduce the turbulence pulsation frequency  $\nu_t$ . When the turbulence frequency exceeds the binary collision frequency, it is precisely the turbulence frequency that should enter the expressions for energy transfer coefficients. We note that the scale of turbulent pulsation is defined as  $l_p = c/\nu_t$  ( $c$  is the speed of light),  $l_p \approx d$  being the typical pore size.

### 3. Simulation results

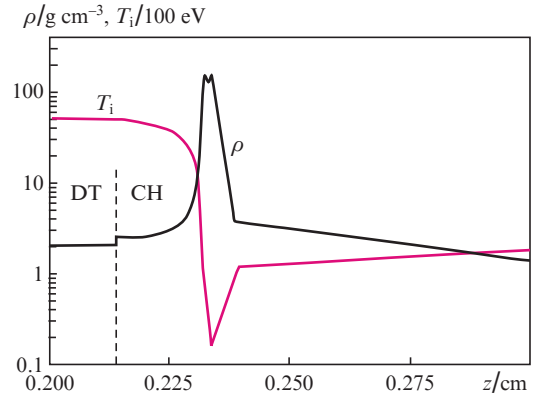
The parameters of the problem were so selected that the time of highest DT fuel compression coincides with the laser pulse duration  $\tau_L$  or was slightly longer and the neutron yield  $Y_n \geq 10^{17}$ . In this case, the radii ratio  $R_1/R_{\min} \approx 20$ .

Figure 4 shows the results of target compression simulations at the point in time  $t_{\text{col}} = 100$  ns (the instant of collapse). The initial target parameters were as follows:  $R_{\min} = 0.1$  cm,  $R_2 = 0.25$  cm,  $R_1 = 2$  cm,  $R_0 = 2.1$  cm,  $\Delta_{\text{CH}} = 55$   $\mu\text{m}$  (the first simulation series). At that point in time the neutron yield  $Y_n$  amounted to  $9 \times 10^{16}$ , the density of compressed fuel  $\rho \approx 4$ – $5$   $\text{g cm}^{-3}$ , and the ion temperature  $T_i \approx 7$  keV. Subsequently the neutron yield rose to  $1.4 \times 10^{17}$ .



**Figure 4.** Density  $\rho$  and ion temperature  $T_i$  distributions along channel axis  $O_1O_2$  at the instant of collapse  $t_{\text{col}} = 100$  ns. The vertical dashed line is the boundary between the DT fuel and the tamper.

Figure 5 depicts the results of target compression simulations at the point in time  $t_{\text{col}} = 253$  ns. The initial parameters target parameters were as follows:  $R_{\min} = 0.2$  cm,  $R_2 = 0.28$  cm,  $R_1 = 4.0025$  cm,  $R_0 = 4.25$  cm,  $\Delta_{\text{CH}} = 55$   $\mu\text{m}$  (the second simulation series). In this version, the instant of highest compression ( $t_{\text{col}} = 253$  ns) occurred somewhat later than



**Figure 5.** Density  $\rho$  and ion temperature  $T_i$  distributions along channel axis  $O_1O_2$  at the instant of collapse  $t_{\text{col}} = 253$  ns. The vertical dashed line is the boundary between the DT fuel and the tamper.

the pulse termination ( $\tau_L = 251$  ns). In this case, the neutron yield  $Y_n$  amounted to  $5 \times 10^{16}$ , the density of compressed fuel  $\rho \approx 2$   $\text{g cm}^{-3}$ , and the ion temperature  $T_i \approx 5$  keV\*. The total neutron yield  $Y_\infty = 1.05 \times 10^{17}$ .

It is therefore possible, in principle, to achieve a neutron yield  $Y_n \approx 10^{17}$  in the one-dimensional approximation with the use of only one long laser pulse. However, the real situation is more complicated. At the stage of tamper deceleration and reflected shock propagation, the pressure of the fuel rises by several orders of magnitude (Fig. 6). Any material (including gold and uranium) will begin to move under the action of such pressures.

Figure 6 shows the pressure distribution in the DT fuel at the stage of tamper deceleration and reflected shock propagation at different points in time. For the sake of convenience of data presentation, plotted on the abscissa in one of the pictures is the mass coordinate in arbitrary units. During this period the internal energy of the fuel amounts to 50–60 kJ and the pressure is equal to 1–10 Gbar.

The sequence of short pulses with a total energy of 50–60 kJ and a duration of 0.1–1 ns, which are injected into the target through the openings located near the cone summits, must fulfil two functions: exert counterpressure at the fuel–wall interface for  $\sim 1$  ns and additionally heat the thermonuclear fuel.

It is pertinent to note that the scheme of additional heating of compressed thermonuclear fuel by a short laser pulse was discussed, supposedly for the first time, in a popular paper by L.P. Feoktistov [18]. Subsequently, with the development of ultrashort laser pulses, there formed a new avenue of research in laser fusion, which came to be known as fast ignition [19].

To produce counterpressure near the walls and confine the fuel, we propose a target design at the cone summits depicted in Fig. 7. At the summit of the target with counter-directed channels there are openings for the injection of short pulses. An aerogel and a foil with a relief permit compensating the pressure nonuniformity at the fuel boundary. The use of a low-density substance and corrugated shells was numerically simulated for open targets in Ref. [20] and for laser

\* By shortening  $R_{\min}$  it is possible to raise the compression ratio and the temperature  $T_i$ , but the probability of mixing with the tamper material and target walls increases in this case.

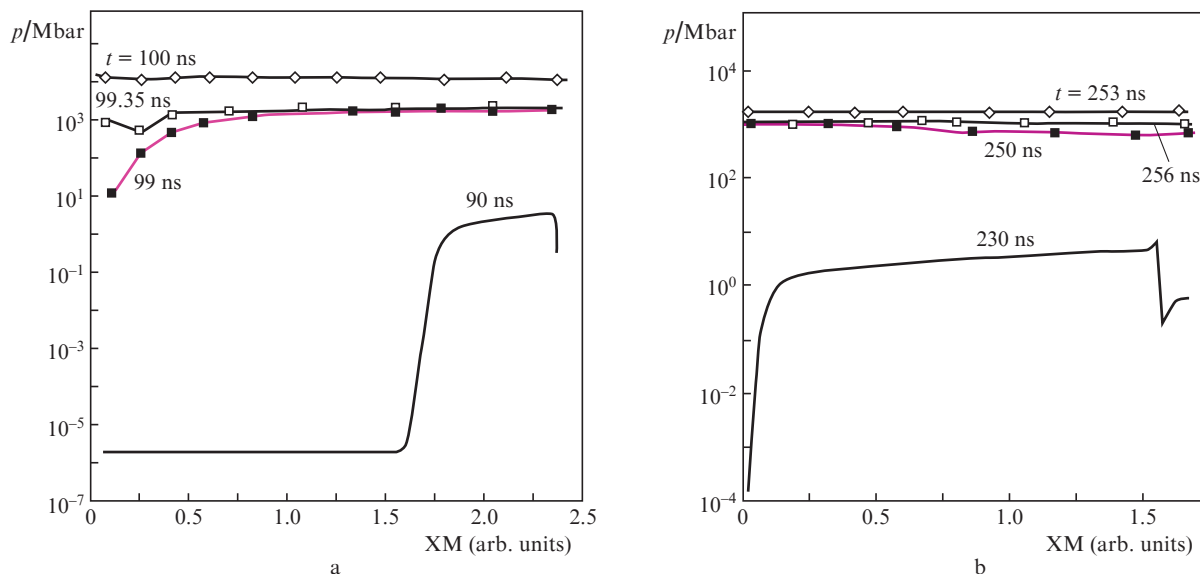


**Figure 6.** Axial distribution of the DT pressure at different points in time obtained in (a) the first and (b) second series of simulations. Plotted on the abscissa are mass coordinates (XM).

greenhouse-type targets in Ref. [21]. The aerogel serves yet another function. As noted earlier [15, 22, 23], spontaneous magnetic fields of  $\sim 10$ – $100$  MGs may be generated in the plasma produced in the irradiation of a porous medium by high-power laser pulses. These fields are responsible for magnetisation of the electron thermal flux to the target walls and, partly, for the increase in the energy fraction which  $\alpha$  particles transfer to the plasma.

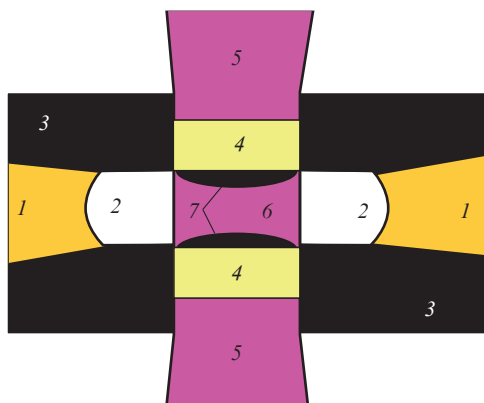


**Figure 7.** Target structure near the cone summits: (1) beams of long laser pulses, which accelerate tampers (2) towards the cone summits; (3) walls of the target with conic channels; (4) low-density aerogel placed in the openings intended for the injection of short pulses (5); (6) condensed DT mixture; (7) gold or uranium thin film with a relief.

The problem considered in the present work is inherently three-dimensional and is characterised by different time scales (the tamper is accelerated in 100–250 ns and is decelerated in  $\sim 1$  ns). The problem of counterpressure formation and compressed fuel confinement will therefore be treated in a separate paper.

#### 4. Discussion of the simulation results and the feasibility of experimental verification of separate propositions of the proposed conception

One can see from the simulation data that it is possible to accelerate a thin dense layer up to  $\sim 300$  km  $s^{-1}$  inside a conic channel with the use of a UV laser pulse with an energy of  $\sim 1$  MJ and a duration of 100–250 ns. Densities of 2–8 g  $cm^{-3}$  and temperatures of  $\sim 5$ –7 keV are achieved in the collision. This permits, in principle, to consider the feasibility of making a high-power source of thermonuclear neutrons. However, several problems remain to be solved:

- the stability of tamper's flight inside the channel and the physics of the interaction of dense accelerated plasma with the channel wall;
- the effect of plasma non-ideality and reradiation;
- generation of spontaneous magnetic fields in the plasma;
- description of the physical processes of compressed plasma confinement; and
- development of hydrodynamic instability and mixing at the channel wall–fuel interface.

The problems listed above are highly complicated from the standpoint of their computer simulation and invite a serious verification of separate propositions of the proposed conception using the existing laser facilities. In our country there is a KrF laser (Garpun) with a pulse energy of about 100 J and a duration of 100 ns. A comparison of numerical simulation data and experimental data [24–26] suggests that laser-driven acceleration of thin foils can impart a velocity of the order of the orbital velocity (5–8) km  $s^{-1}$ ; also discussed was the possibility of making a laser-driven shock tube on the basis of this facility. The facility upgrade and the development of an additional channel delivering a short  $\sim 1$ -ps pulse with an energy of  $\sim 1$  J (the facility received the name Garpun-MTW [27]) furnished the possibility of investigating the injection of short laser pulses through openings, energy transfer, and production of high pressures in an aerogel.

The authors of Ref. [23] proposed two approaches to the experimental investigation of magnetic fields in the plasma produced by laser irradiation of low-density porous targets. These experiments may be performed on the Garpun-MTW facility.

There is a possibility of carrying out a full-scale experiment on the NIF facility (USA), where use is made of the corresponding experimental target irradiation scheme (two-sided scheme with pulse timing) and there is a short pulse of sufficiently high energy along with the long pulse ( $\tau_L = 10\text{--}20$  ns). According to our estimates, the neutron yield for such targets might be equal to  $\sim 10^{16}$  per pulse, i.e. be comparable to the yield observed in indirect drive experiments.

## 5. Conclusions

Therefore, the following results were obtained in the present work:

1. The heating and compression of two-sided conical targets by 100–250 ns long KrF laser pulses was investigated by numerical simulation techniques.
2. We showed that a high-power thermonuclear neutron source with a yield of  $\sim 10^{17}$  per pulse can be made using such targets and laser facilities with a pulse energy of  $\sim 1$  MJ.
3. Such neutron sources were determined to hold much promise for a hybrid nuclear-thermonuclear reactor.

## References

1. Garanin S.G., Bel'kov S.A., Bondarenko S.V. *Proc. XXXIX Intern. (Zvenigorod) Conf. on Plasma Phys. and Controlled Fusion* (Zvenigorod, 6–10 February, 2012) p. 17; Belkov S.G., Garanin S.G., Shagalkin Yu.V. [http://plasma.mephi.ru/ru/uploads/files/conferences/ECLIM2016/Presentations/ECLIM%202016\(eng\)%20S%20A%20Belkov.pdf](http://plasma.mephi.ru/ru/uploads/files/conferences/ECLIM2016/Presentations/ECLIM%202016(eng)%20S%20A%20Belkov.pdf).
2. Moses E.I. *Nucl. Fusion*, **53**, 104020 (2013).
3. Obenschain S., Lehmberg R., Kehne D., Hegeler F., Wolford M., Sethian J., Wever J., Karasik M. *Appl. Opt.*, **54** (31), 103 (2015).
4. Basov N.G., Belousov N.I., Grishunin P.A., Kalmykov Yu.K., Lebo I.G., Rozanov V.B., Sklizkov G.V., Subbotin V.I., Finkil'shtein K.I., Kharitonov V.V., Sherstnev K.B. *Sov. J. Quantum Electron.*, **17** (10), 1324 (1987) [*Kvantovaya Elektron.*, **14** (10), 2068 (1987)].
5. Basov N.G., Subbotin V.I., Feoktistov L.P. *Vestn. Ross. Akad. Nauk*, **63**, 878 (1993).
6. Lebo I.G. *Quantum Electron.*, **30** (5), 409 (2000) [*Kvantovaya Elektron.*, **30** (5), 409 (2000)].
7. Basov N.G., Lebo I.G., Rozanov V.B., Tishkin V.F., Feoktistov L.P. *Quantum Electron.*, **28** (4), 316 (1998) [*Kvantovaya Elektron.*, **25** (4), 327 (1998)].
8. Lebo I.G., Tishkin V.F. *Issledovanie gidrodinamicheskoi neustoiichivosti v zadachakh lazernogo termoyadernogo sinteza metodami matematicheskogo modelirovaniya* (Investigation of Hydrodynamic Instabilities in Laser Fusion Problems by Mathematical Simulation Techniques) (Moscow: Fizmatlit, 2006).
9. Kuzenov V.V., Lebo A.I., Lebo I.G., Ryzhkov S.V. *Fiziko-matematicheskie modeli i metody rascheta moshchnykh lazernykh i plazmennykh impul'sov* (Physicomathematical Models and Simulation Methods of the Action of High-Power Laser and Plasma Beams) (Moscow: Izd. MG TU im. N.E. Bauman, 2015).
10. Dolgoleva G.V., Lebo A.I., Lebo I.G. *Mat. Model.*, **28** (1), 23 (2016).
11. Zvorykin V.D., Lebo I.G. *Laser Part. Beams*, **17**, 69 (1999).
12. Braginskii S.I., in *Reviews of Plasma Physics*. Ed. by M.A. Leontovich (New York: Consultants Bureau, 1963; Moscow: Atomizdat, 1963) Vol. 1.
13. Konash P.V., Lebo I.G. *Quantum Electron.*, **36** (8), 767 (2006) [*Kvantovaya Elektron.*, **36** (8), 767 (2006)].
14. Lebo A.I., Lebo I.G. *Mat. Model.*, **21** (1), 75 (2009).
15. Lebo A.I., Lebo I.G. *Mat. Model.*, **21** (11), 16 (2009).
16. Lebo I.G., Lebo A.I. *Phys. Scripta*, **T142**, 014024 (2010).
17. Belen'kii S.Z., Fradkin E.S. *Tr. Fiz. Inst. Akad. Nauk SSSR*, **29**, 207 (1965).
18. Feoktistov L.P., in *Budushchee nauki* (The Future of Science) (Moscow: Znanie, 1985) pp 168–182.
19. Tabak M., Hammer J., Glynsky M.E., Kruer W.L., et al. *Phys. Plasmas*, **1**, 1636 (1994).
20. Lebo I.G., Rozanov V.B., Tishkin V.F. *Laser Part. Beams*, **12** (3), 361 (1994).
21. Lebo I.G., Popov I.V., Rozanov V.B., Tishkin V.F. *Quantum Electron.*, **25** (12), 1220 (1995) [*Kvantovaya Elektron.*, **22** (12), 1257 (1995)].
22. Konash P.V., Lebo A.I., Lebo I.G. *Mat. Model.*, **25** (6), 3 (2013).
23. Lebo I.G., Lebo A.I. *Vestn. MG TU MIREA (MSTU MIREA Herald), Electronic Internet Scientific and Methodical Journal*, **3** (4), 215 (2014) (<https://www.mirea.ru/science/vestnik-mirea>).
24. Bakaev V.G., Batani D., Krasnyuk I.A., Lebo I.G., Levchenko A.O., Sychugov G.V., Tishkin V.F., Zayarnyi D.A., Zvorykin V.D. *J. Phys. D: Appl. Phys.*, **38**, 2031 (2005).
25. Lebo I.G., Zvorykin V.D. *Phys. Scripta*, **T132**, 016018 (2008).
26. Zvorykin V.D., Lebo I.G. *Quantum Electron.*, **30** (6), 540 (2000) [*Kvantovaya Elektron.*, **30** (6), 540 (2000)].
27. Zvorykin V.D., Didenko N.V., Ionin A.A., Kholin I.V., et al. *Laser Part. Beams*, **25**, 435 (2007).